NMR-Solution Structures in Methanol of an α-Heptapeptide, of a β^3/β^2-Nonapeptide, and of an all-β^3-Icosapeptide Carrying the 20 Proteinogenic Side Chains

by **Dieter Seebach***, **Raveendra I. Mathad**[1]), **Thierry Kimmerlin**[2]), **Yogesh R. Mahajan**, **Pascal Bindschädler**[3]), **Magnus Rueping**, and **Bernhard Jaun***

Laboratorium für Organische Chemie der Eidgenössischen Technischen Hochschule, ETH-Hönggerberg, Wolfgang-Pauli-Strasse 10, HCI, CH-8093 Zürich

and

Christian Hilty and **Touraj Etezady-Esfarjani**

Institut für Molekularbiologie und Biophysik der Eidgenössischen Technischen Hochschule ETH-Hönggerberg, Schafmatt-Strasse 20, HPK, CH-8093 Zürich

Herrn Professor *Rolf Huisgen* zum 85. Geburtstag gewidmet

The NMR-solution structure of an α-heptapeptide with a central Aib residue was investigated in order to verify that, in contrast to β-peptides, short α-peptides do not form a helical structures in MeOH. Although the central Aib residue was found to induce a bend in the experimentally determined structure, no secondary structure typical for longer α-peptides or proteins was found. A β^2/β^3-nonapeptide with polar, positively charged side chains was subjected to NMR analysis in MeOH and H_2O. Whereas, in MeOH, it folds into a *10/12*-helix very similar to the structure determined for a corresponding β^2/β^3-nonapeptide with only aliphatic side chains, no dominant conformation could be determined in H_2O. Finally, the NMR analysis of a β^3-icosapeptide containing the side chains of all 20 proteinogenic amino acids in MeOH is described. It revealed that this 20mer folds into a 3_{14}-helix over its whole length forming six full turns, the longest 3_{14}-helix found so far. Together, our findings confirm that, in contrast to α-peptides, β-peptides not only form helices with just six residues, but also form helices that are longer than helical sections usually observed in proteins or natural peptides. The higher helix-forming propensity of long β-peptides is attributed to the conformation-stabilizing effect of the staggered ethane sections in β-peptides which outweighs the detrimental effect of the increasing macrodipole.

1. Introduction. – The surprising stability in solution of secondary structures such as helices and hair-pin turns of short β- and γ-peptides carrying the side chains of proteinogenic α-amino acids has been amply demonstrated (see the discussion in a recent review article [1]). Still, there remain several important questions to be answered. Three of them are outlined as follows.

i) We have always claimed that comparable α-peptides consisting of less than ten amino-acid residues do not fold to a helix under the same conditions we used to detect the folding of their counterparts containing homologated amino acids (NMR analysis of solutions in MeOH). When looking at the huge body of investigations by *Baldwin et al.* at Stanford ('single domain proteins') [2–4], this claim appears to be reasonable, but we have actually not found a report on an NMR-structural study of a short α-

[1]) Part of the projected Ph.D. Thesis of *R. I. M.*, ETH-Zürich.
[2]) Part of the Ph.D. Thesis of *T. K.*, Dissertation Nr. 15800, ETH-Zürich, 2004.
[3]) Part of the Master Thesis (Diplomarbeit) of *P. B.,* ETH-Zürich, 2003.

peptide in MeOH (a helix-stabilizing solvent!). Thus, we have now prepared the α-heptapeptide **1** with a central, helix-inducing Aib residue and analyzed its structure by NMR spectroscopy in this solvent. A previous simulation of **1** by the GROMOS molecular-modeling program package had provided no evidence for a secondary structure in MeOH [5].

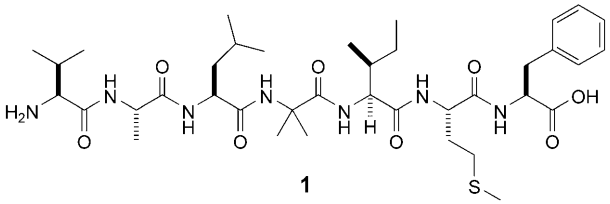

1

ii) β-Peptides consisting of simple homologated α-amino acids can form two types of helices, the 3_{14} (β^2- or β^3-) and the $2.6_{10/12}$ (β^2/β^3)-helix, depending on the substitution pattern on the peptide backbone. The 3_{14}-helix has been studied thoroughly with all kinds of helix-stabilizing and -destabilizing side-chain arrangements [1], but we have so far only determined NMR structures of *10/12*-helices with aliphatic, hydrophobic, and non-polar side chains [6–8]. The preparation [9] and tests for antibiotic and haemolytic activities [10] of the β^2/β^3-nonapeptide **2** with two lysine side chains, positioned such that an amphipathic *10/12*-helix should result, have been published recently. CD Measurements indicate that this peptide may indeed, fold to a *10/12*-helix in MeOH and loose its secondary structure in H_2O, with increasing pH value of the solution (3.5, 7.0, 11.0) [9]. We now report its NMR structure in MeOH solution and a comparison of the spectra in MeOH and in H_2O.

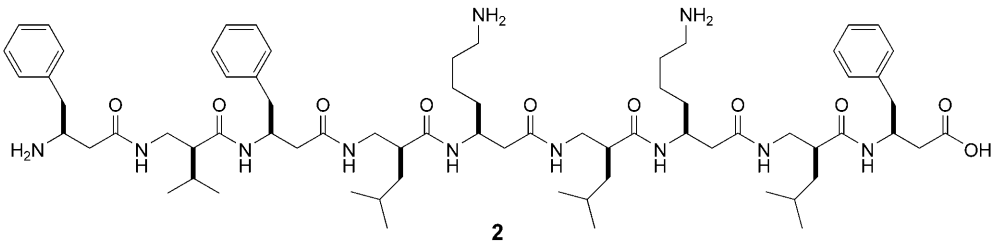

2

iii) Two years ago, we have published the synthesis, and characterization by HPLC analysis, CD, and routine NMR spectroscopy, and high-resolution mass spectrometry of the all-β^3-icosapeptide **3** containing the 20 homologated proteinogenic amino acids, *i.e.*, with no two identical amino acid residues in the chain, to facilitate a complete NMR-structure elucidation [11]. Furthermore, this peptide was constructed such that a helical secondary structure would be stabilized by two salt bridges (β^3hGlu$^6 \rightarrow \beta^3$hArg^9 and β^3hAsp$^{11} \rightarrow \beta^3$hLys^{14}).

H-β^3hCys-β^3hAla-β^3hSer-β^3hHis-β^3hAsn-β^3hGlu$^{\ominus}$-β^3hGly-β^3hTrp-β^3hArg$^{\oplus}$-β^3hVal-

-β^3hAsp$^{\ominus}$-β^3hGln-β^3hIle-β^3hLys$^{\oplus}$-β^3hThr-β^3hLeu-β^3hTyr-β^3hMet-β^3hPro-OH

3

Also, a helix of peptide **3** would be amphipathic, having stripes of polar and non-polar side chains along its surface. A full helix along the entire length of the 20-mer, *i.e.*, almost seven turns (of *ca.* 5-Å pitch) and a total length of over 30 Å (3 nm!) would have a large resulting dipole. Such macro-dipoles are known to destabilize helices of α-peptides, an effect which is counteracted by negatively charged side chains near the positive end and by positively charged side chains near the negative end of the dipole in many helices of proteins and enzymes ('capping')[4] [2][13]. When going from α- to β-peptidic helices, there is a reversal of the dipole direction with respect to the helix *termini*. The $\oplus$-pole of the natural helix is at the *N-terminus*, which is positively charged (NH_3^+), and the $\ominus$-pole is at the negatively charged *C-terminus*, causing additional destabilization. In contrast, the C=O dipoles in the β-peptidic helix are oriented from the *C*- towards the *N-terminus*, so that this helix has an inherent 'capping' stabilization. The fact that the 3_{14}-helix of β-peptides is more stable with unprotected than with protected *termini* [6–8][14] is evidence for this phenomenon. For a schematic presentation of the various effects in the two helices, see *Fig. 1*.

The β-icosapeptide **3** has no 'capping' by charged side chains in a helical form, so that we could learn about the helix's inherent stability by a structural analysis. The longest β-peptide, of which an NMR-solution structure has been determined, is a dodecamer [15][5]). For longer β-peptides, there is only indirect controversial, and not very reliable [1][17], evidence from CD spectra for the presence of helices in solution [18][19].

2. Preparation of the Peptides 1–3. – The α-heptapeptide **1** was prepared on an Fmoc-L-Phe-*Wang* resin with an automated *ABI 433* peptide synthesizer [20]. The amino acid building blocks were introduced with a 'double-couple' procedure by using 10 equiv. of building blocks for each coupling, whereby HATU (= *O*-(7-azabenzotriazol-1-yl)-1,1,3,3-tetramethyluronium hexafluorophosphate) was employed as the coupling reagent for Aib and Leu residues, and HOBt (= 1-hydroxy-1*H*-benzotriazole)/HBTU (= *O*-(1*H*-benzotriazol-1-yl)-1,1,3,3-tetramethyluronium hexafluorophosphate) for the remaining amino acids (see *Exper. Part*). The synthesis of the mixed β^3/β^2-nonapeptide **2**, [9] and the β^3-icosapeptide **3** [11] have been described previously. For the mixed β^3/β^2-nonapeptide **2**, we used a strategy designed such that the risk of racemization of the β^2-amino acid building blocks would be minimized: we first prepared in solution, by carbodiimide-mediated coupling, Fmoc-protected β^2/β^3-

---

[4]) The lengths of helices in proteins and enzymes rarely surpasses five turns (18 amino-acid residues in a 3.6_{13} helix). A recent NMR-solution structure of an α-peptidic 25-mer in the strongly helix-inducing solvent CF_3CH_2OH/H_2O shows a helix mainly in the region of residues 7 to 23 [12].

[5]) For the NMR-structure (MeOH, 10°) of a 'capped' and salt-bridge-stabilized β^3-decapeptide, see a recent communication [16].

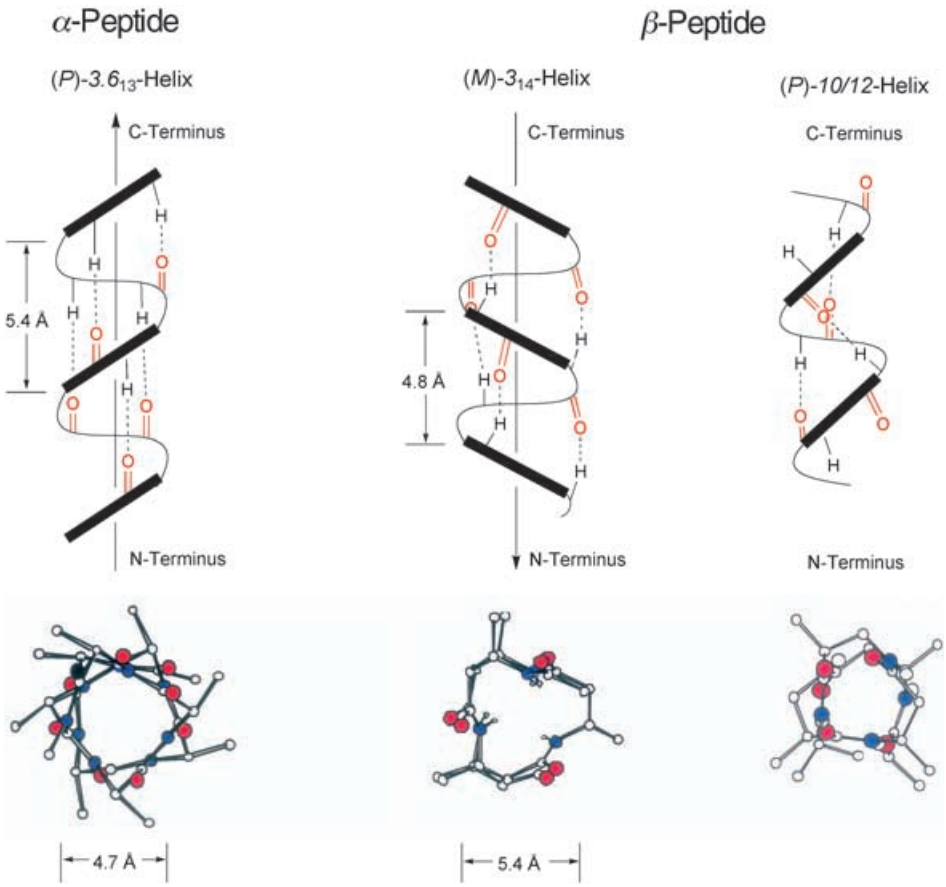

Fig. 1. *Schematic representation of the preferred helical forms of α-peptides* (left), *β^3-peptides* (center), *and β^2,β^3-peptides* (right). The direction of the macrodipole is indicated along the axis.

dipeptides, which were then used as building blocks for the solid-phase synthesis on a *Wang* resin using HOBt/HBTU as the coupling reagent. On the other hand, peptide **3** was prepared by coupling Fmoc-protected *β*^{3}-amino acids on a *Wang* resin using HATU as the coupling reagent and piperidine/DBU for Fmoc deprotection. All three peptides were purified by preparative reverse-phase HPLC and identified by high-resolution mass spectrometry (ESI or MALDI).

3.1. *NMR Analysis of α-Peptide* **1**. A set of standard NMR experiments DQF-COSY, TOCSY, HSQC, HMBC of *α*-peptide **1** in CD_3OH at 500 MHz/125 MHz allowed complete assignment of all ^{1}H- and ^{13}C-resonances (*Table 1*).

The coupling constants ^3J(NH,HC(*α*)) were extracted from the 1D-^{1}H-NMR spectrum. Analysis of the ROESY spectrum showed no NOEs typical of one of the known secondary structures of *α*-peptides. Integration of NOE cross-peak volumes from the 300-ms ROESY spectrum yielded distance restraints (*Table 2*), which were used in slow-cooling-simulated annealing calculations with XPLOR-NIH. Each

Table 1. *^{1}H- and ^{13}C-NMR Data and Assignments for α-Heptapeptide* **1**

α-Amino acid	NH	$CH_2(\alpha)$ (^3J(HN,H_α))	H–C(β)	H–C(γ), Me–C(γ), $CH_2(\gamma)$	H–C(δ), Me–C(δ)	C(α)	C(β)	C(γ)	C(δ)
Val[1]		3.66	2.18	1.04	1.04	59.85	31.73	19.00	
Ala[2]	8.54	4.45 (6.85)	1.38			50.53	17.92		
Leu[3]	8.13	4.22 (6.24)	1.59	1.73	0.95	54.47	41.69	25.80	22.20
Aib[4]	8.17		1.45				25.84/25.20		
Ile[5]	7.29	4.18 (7.70)	1.96	1.22/1.70	0.88	60.01	37.39	26.10	11.60
Met[6]	8.01	4.43 (7.83)	1.94/2.00	2.48		54.12	32.40	31.20	

Table 2. *NOE Distance Restraints for α-Heptapeptide* **1**

Residue	H-Atom[a])	Residue	H-Atom	Distance [Å]	Residue	H-Atom[a])	Residue	H-Atom	Distance [Å]
1	β	1	α	2.5	2	α	3	γ	4.1
1	α	1	γ	3.0	2	α	3	HN	2.1
2	α	2	β	2.5	3	α	2	β	4.0
2	α	2	HN	2.8	3	HN	2	β	3.3
2	β	2	HN	3.1	3	HN	2	HN	4.2
3	β	3	α	2.3	3	α	4	HN	2.1
3	δ	3	α	3.5	3	β	4	HN	3.0
3	γ	3	α	2.7	4	β	5	HN	2.5
3	HN	3	α	2.5	4	HN	5	HN	2.9
3	HN	3	γ	2.8	5	α	6	HN	2.5
3	β	3	HN	2.6	5	HN	6	HN	2.8
4	HN	4	β	3.1	5	HN	4	β	3.0
5	β	5	α	2.4	6	α	7	HN	2.6
5	γ2*	5	α	3.6	6	β	7	HN	3.6
5	γ2*	5	HN	3.6	6	HN	7	HN	3.5
5	HN	5	α	2.8	1	γ	3	HN	5.0
5	HN	5	β	2.6	1	γ	3	α	4.2
5	β	5	γ1*	2.4	2	β	5	β	3.7
5	HN	5	γ1*	3.0	3	α	6	γ	3.6
6	β	6	α	2.5	3	α	6	ε	4.4
6	γ	6	α	2.9	3	β	5	HN	3.7
6	HN	6	α	2.6	3	β	6	γ	3.8
6	HN	6	γ	3.1	3	β	6	HN	4.0
6	HN	6	β	2.7	4	β	6	HN	3.9
7	α	7	β	3.7	4	β	7	β	4.2
7	HN	7	β	3.2	4	β	7	HN	4.7
1	β	2	α	3.6	5	β	2	HN	4.3
1	α	2	β	4.6	5	γ2*	7	HN	4.9
1	α	2	HN	2.2	5	HN	2	β	4.3
1	β	2	HN	3.0	5	HN	3	α	3.4
1	γ*	2	HN	3.8	6	HN	2	β	4.8
1	γ*	2	α	4.2	6	HN	3	α	3.2
1	α	2	α	3.9	6	HN	4	α	3.9
2	α	3	β	4.1	6	ε	3	α	4.4

[a]) γ1* = CH_2, pseudo-atom, γ* and γ2* = Me.

calculation was started with an extended conformer, and a bundle of all calculated structures with neither NOE nor dihedral-angle constraint violations is shown in *Fig. 2*. All calculated structures do show a bend induced by the Aib residue in the middle of the sequence but otherwise, this α-heptapeptide does not assume one of the known canonical secondary structures. Although the bundle of calculated structures appears well defined and does not show any NOE violations, this may be the result of the predominance of sequential NOEs. In contrast to long-range NOEs, such as those determining the central bend, time-averaged sequential NOE constraints from a multiconformational ensemble are more likely to appear consistent with a single (unreal) conformer without violations of the error bounds given by the constraints.

3.2. *NMR Analysis of β^3,β^2-Nonapeptide* **2**. A comprehensive NMR study of **2** in CD_3OH and H_2O/D_2O was carried out at 750 MHz. Complete assignment of all ^{1}H-resonances was achieved through COSY and TOCSY, and, for the sequential assignments, NOESY spectra (see *Table 3*). NOESY Spectra were recorded with mixing times of 150 and 400 ms, and, for H_2O/D_2O, with 150 ms. Qualitative analysis of the NOESY spectrum in CD_3OH showed the typical NOEs for a *10/12*-helical structure. NOE Cross-peak volumes from the spectrum with 400-ms mixing time were integrated and converted to distance restraints (*Table 4*). Together with dihedral angle

Fig. 2. *Bundle of 30 structures with no NOE or dihedral-angle constraint violations calculated for α-peptide* **1**. Superposition based on the backbone atoms of the central Aib residue.

Table 3. *^{1}H-NMR Data and Assignments for β^3,β^2-Nonapeptide* **2**

β-Amino acid	NH	$CH_2(\alpha)$	H–C(β) (^3J(HN,H$_\beta$))	H–C(γ), Me–C(γ), $CH_2(\gamma)$	H–C(δ), Me–C(δ)
β^3hPhe[1]		2.86	3.81	2.91, 3.01	
β^2hVal[2]	8.18	1.94	2.90, 3.78	1.57	0.84
β^3h Phe[3]	8.24	2.02	4.64 (9.15)	2.68, 2.89	
β^2hLeu[4]	8.54	2.49	2.78/3.48	0.98, 1.54	1.48
β^3hLys[5]	8.77	2.25, 2.70	4.45 (9.16)	1.42, 1.54	
β^2hLeu[6]	8.55	2.51	2.88/2.63	1.12, 1.68	1.58
β^3hLys[7]	8.73	2.11, 2.55	4.36 (9.15)	1.51, 1.64	
β^2hLeu[8]	7.99	2.38	2.92/3.42	0.89, 1.42	1.00
β^3hPhe[9]	8.58	2.55, 2.63	4.61 (8.70)	2.72, 2.94	

Table 4. *NOE Distance Restraints for β^2,β^2-Nonapeptide* **2**

Residue	H-Atom	Residue	H-Atom	Distance [Å]	Residue	H-Atom	Residue	H-Atom	Distance [Å]
2	β	2	α	2.8	8	β	8	HN	2.9
2	HN	2	α	3.0	8	α	8	γ	2.8
2	β	2	HN	3.1	9	α	9	HN	2.7
2	β	2	γ	2.9	9	β	9	HN	2.9
2	γ	2	α	3.2	9	γ	9	HN	2.9
3	α	3	HN	3.0	1	α	2	HN	2.9
3	β	3	HN	3.0	2	α	3	HN	2.4
3	β	3	α	2.6	3	α	4	HN	2.9
3	α	3	γ	2.7	4	α	5	HN	2.3
4	α	4	β	2.6	4	HN	5	HN	3.1
4	α	4	γ	2.7	5	α	6	HN	2.8
4	β	4	HN	2.9	5	β	6	HN	2.8
5	β	5	α	2.6	6	α	7	HN	2.3
5	HN	5	α	3.0	6	HN	7	HN	3.0
5	β	5	γ	2.8	7	α	8	HN	2.5
5	β	5	HN	2.9	7	α	6	HN	3.4
5	HN	5	γ	2.8	7	β	8	HN	3.0
6	α	6	γ	2.8	8	α	9	HN	2.3
6	α	6	HN	2.7	8	HN	9	HN	3.4
6	β	6	HN	2.8	2	HN	4	α	3.2
7	α	7	β	2.9	2	HN	5	HN	4.0
7	HN	7	α	2.9	3	β	5	α	2.8
7	β	7	γ	2.8	3	β	5	HN	2.9
7	β	7	HN	2.9	4	β	2	HN	3.7
7	γ	7	HN	2.8	5	β	7	α	2.8
8	α	8	β	2.9	5	β	7	HN	2.9
8	α	8	HN	3.3	7	β	9	HN	3.0

constraints derived from coupling constants, the distance restraints were used in slow-cooling-simulated annealing calculations (SA) with XPLOR-NIH. Starting with an extended zigzag conformer, a total of 30 structures were calculated. A bundle of the 20 structures with the lowest energy and no NOE or dihedral angle constraint violations is shown in *Fig. 3*,*a*. The unprotected β^3,β^2- peptide **2** in MeOH solution adopts a $2.6_{10/12}$-helical conformation, which is characterized by alternating ten- and twelve-membered H-bonded rings from NH_i (where $i \geq 2$) to C=O($i+1$) (*Fig. 3*,*b*), completely analogous to the structure of the β^3,β^2-peptide with only aliphatic side chains[6]) as illustrated by the single structure (in cyan) superimposed over the bundle for **2** in *Fig. 3*,*a*. The corresponding *N*-Boc-protected β^3,β^2-peptide[7]) exhibits an additional twelve-membered H-bonded ring at the N-terminus because, in this case, the NH of the Boc group also serves as a H-bond donor to the carbonyl O-atom of residue 2 [8].

In the ^{1}H-NMR spectrum of β^3,β^2-nonapeptide **2** in H_2O/D_2O 9 :1 (data not shown), the NH signals appear within a narrower range of chemical shifts and are shifted to higher field compared with the spectrum in CD_3OH. The HN,HC(β) coupling constants of the β^3-residues are larger (*ca.* 9 Hz) and comparable to those in MeOH, whereas, for

6) See compound **5d** in [8].
7) See compound **5a** in [8].

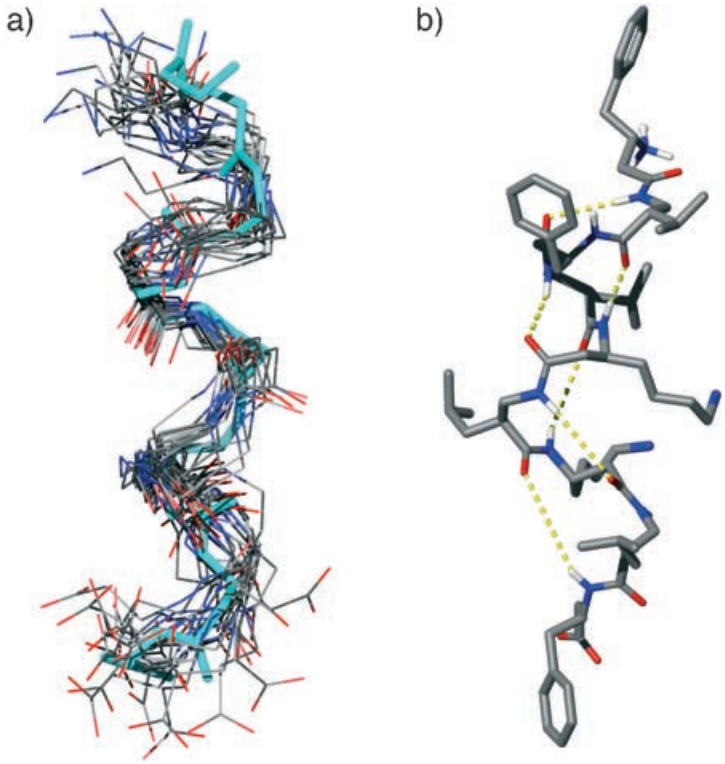

Fig. 3. *NMR Structure of the β^2/β^3-nonapeptide* **2**. *a*) Bundle of the 20 structures with lowest energy and no NOE or dihedral constraint violations. The single structure displayed in cyan was calculated for a corresponding nonapeptide with only aliphatic side chains [8]. Superposition based on the backbone atoms of residues 2–8. The side chains are omitted for clarity. *b*) A single structure from the bundle displayed in *Fig. 3*, *a*, illustrating the alternating ten- and twelve-membered H-bonded rings.

the β^2-residues, the ^3J(HN,H2C(β)) values are equal for the two diastereotopic β-H-atoms (2 × *ca.* 5.5 Hz) and close to the averaged values of a 'random-coil' peptide. All ^{1}H-resonances could be assigned from the COSY, TOCSY, and NOESY spectra. Qualitative comparison of cross-peak volumes in the NOESY spectra (150 ms) in MeOH and H_2O showed that long-range NOEs ($i \rightarrow i+2/i+3$) are much weaker and exhibit a different pattern in H_2O. Most sequential and intraresidual NOEs were present in both solvents, although with different relative intensities. The reduced dispersion of chemical shifts of the NH protons, the coupling constants and the NOE pattern, together, indicate that, in water, β^3,β^2-nonapeptide **2** does not assume a single dominant conformation. This observation is consistent with the changes observed in the CD spectra of **2** when the solvent was changed from MeOH to H_2O at pH 7 [9].

3.3. *NMR Analysis of β^3-Icosapeptide* **3**. To determine the secondary structure of β-icosapeptide **3**, a full NMR analysis in CD_3OH was carried out at 750 MHz/ 187 MHz. The 1D-^{1}H-NMR showed good dispersion of the signals from the backbone H-atoms, indicating the presence of a regular secondary structure. The amino-acid spin systems

could be fully assigned by a combination of DQF-COSY and TOCSY techniques, whereas sequence assignment was derived from $d_{\alpha,N}(i,i+1)$ and $d_{N,N}(i,i+1)$ sequential NOEs and (in part) HSQC/HMBC correlations (*Table 5*). The large coupling constants (*ca.* 9 Hz for $^3J(NH,C_\beta H)$), which were extracted from ^{1}H-NMR, correspond to an antiperiplanar arrangement of NH and H_β. The diastereotopic $CH_2(\alpha)$ H-atoms were assigned assuming that the axial[8]) H-atoms exhibit a large, and the lateral H-atoms a small coupling with $H-C(\beta)$. This is in agreement with stronger NOEs being observed from $H-C(\beta)$ to the lateral $H_{lat}-C(\alpha)$ H-atoms, compared with the axial $H_{ax}-C(\alpha)$ H-atoms, and stronger NOEs from $H_{ax}-C(\alpha)_i$ to the NH_{i+1} H-atoms.

Table 5. *^{1}H-NMR Data and Assignments for β^3-Icosapeptide* **3**

β^3-Amino acid	NH	$CH_2(\alpha)$	$H-C(\beta)$ ($^3J(HN,H_\beta)$)	$H-C(\gamma)$, $Me-C(\gamma)$, $CH_2(\gamma)$	$H-C(\delta)$, $Me-C(\delta)$	$Me-C(\varepsilon)$
β^3hCys[1]		2.86, 2.97	4.002	3.07, 2.11		
β^3hAla[2]	8.21	2.84	4.57	1.25		
β^3hSer[3]	8.62	2.48, 2.93	4.31	3.56		
β^3hHis[4]	8.54	2.57, 2.76	4.66	2.82, 2.95		
β^3hAsn[5]	8.33	2.59, 2.89	4.75	2.15, 2.40		
β^3hGlu[6]	8.23	2.47, 2.87	4.56	1.85		
β^3hGly[7]	8.68	2.38, 3.09	2.887 (4.05)			
β^3hTrp[8]	8.63	2.61, 3.02	4.70	3.0, 3.1		
β^3hArg[9]	8.53	2.54, 2.92	4.50	1.76	1.64	3.15, 3.21
β^3hVal[10]	8.39	2.53, 2.83	4.32	1.84	0.99, 1.02	
β^3hAsp[11]	8.47	2.75	5.14	2.85, 2.98		
β^3hGln[12]	8.60	2.53, 3.03	4.55	1.82, 2.00		
β^3hIle[13]	8.03	2.74, 2.75	4.29	1.48	0.94, 1.09	
β^3hLys[14]	8.24	2.61, 2.93	4.55	1.70	1.19	1.77
β^3hThr[15]	8.14	2.87	4.51	3.85	1.19	
β^3-hLeu[16]	8.16	2.39, 2.53	4.56	1.37, 1.51	1.69	0.95, 0.97
β^3hTyr[17]	7.92	2.34, 2.47	4.59	2.69		
β^3hMet[18]	7.53	2.25, 2.47	4.59			
β^3hPhe[19]	7.74	2.48, 2.63	4.68	2.81, 2.91		
β^3hPro[20]	–	2.88	4.37	2.076	1.91, 1.95	3.41, 3.50

To determine the three-dimensional structure of peptide **3**, NOESY spectra at different mixing times (150 and 400 ms) were acquired. Examination of the NOE patterns showed that all cross peaks characteristic for 3_{14}-helical conformations were present. The cross-peak volumes of the NOESY spectrum with $t_m = 400$ ms were converted into the distance restraints (see *Exper. Part*) and calibrated with known distances on the basis of the two-spin approximation (*Table 6*). Together with dihedral-angle constraints derived from the coupling constants, the distance restraints were used in simulated-annealing (SA) molecular-dynamics calculations of structural bundles for **3** with XPLOR-NIH. Starting with a randomized conformer, all 30 structures calculated by SA converged to a single cluster with no NOE and dihedral angle violations. The bundle of the 30 structures with the lowest energy displayed in *Fig. 4* reveals that the molecule assumes a 3_{14}-helical conformation over its whole length, although the backbone is less well-defined for the two terminal residues because of a low density of NOEs at the ends of the sequence. Compared with shorter 3_{14}-helical β-hexa- and β-

[8]) *Axial* are the H-atoms of C–H bonds, which are in an approximately parallel orientation with respect to the helix axis, *lateral* are the ones pointing in a perpendicular direction [1].

heptapeptides observed earlier, the bundle obtained for β-icosapeptide **3** has a larger rmsd value of the backbone. In fact, the individual structures in the bundle vary in total length (as measured from the N-terminal N-atom to the C-terminal carboxy C-atom) from 25 to 34 Å. This variation is a consequence of the limited range of the detectable NOEs (i to max. $i+3$), which leads to an accumulation of small errors along the full length of the 20-mer. Whereas our NOE data leave no doubt that the secondary structure of this β-icosapeptide is an uninterrupted 3_{14}-helix, the local conformation in the side chains is not well-defined by the experimental data. In particular, only one of the two salt bridges built into the sequence by design is corroborated by a weak NOE between the side chains of β^3hAsp^{11} and β^3hLys^{14}.

4. Conclusions. – The NMR analysis in MeOH of the α-heptapeptide **1** with hydrophobic side chains – and a helix-inducing central Aib residue – confirms that, under the same conditions, α-peptides have a much weaker propensity for folding to a

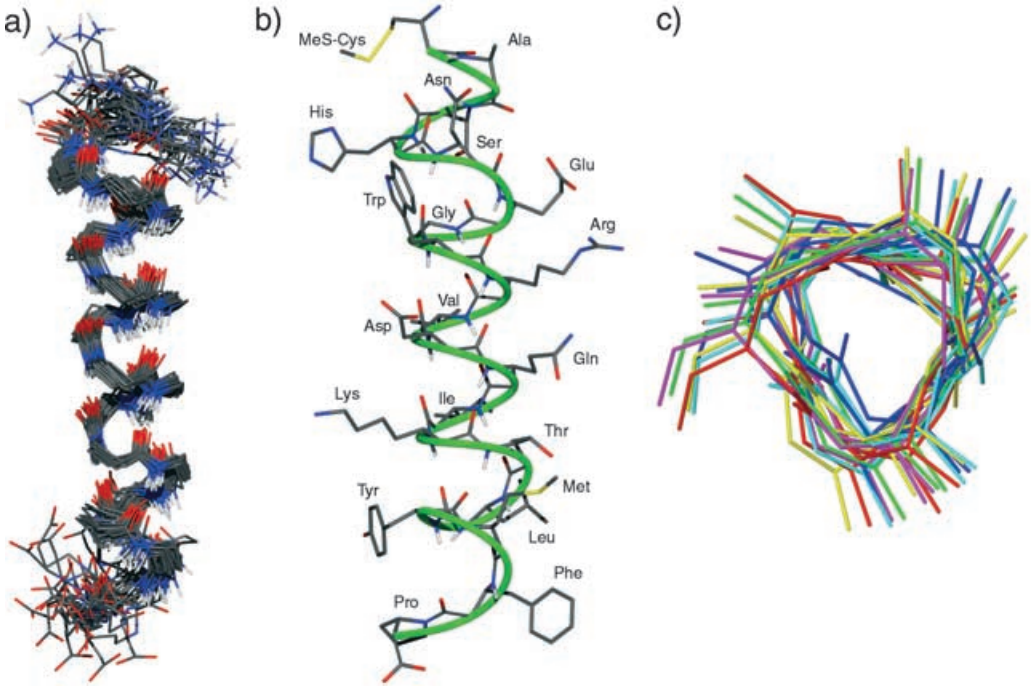

Fig. 4. *NMR Structure of the β^3-icosapeptide* **3**. *a*) Bundle of the 20 structures with lowest energy and no NOE or dihedral constraint violations. Superposition based on the backbone atoms of residues 2 – 19. The side chains are omitted for clarity. *b*) Single structure from the bundle shown in *Fig. 4,a* illustrating the almost six full turns of the 3_{14}-helix with labels for the 20 different proteinogenic side chains. *c*) View along the axis of the (*M*)-helix section containing residues 8 – 14; side chains (only C(γ) shown) in i and ($i+3$)-positions are offset from an ideal 3_{14}-helix by 10° to 20° per turn in a right handed direction; thus, there are 3.1 to 3.4 residues per turn. Taking the six structures lowest in energy, an average pitch of 4.8 Å can be assigned, and cylinders least-squares-fit through the CO and through the C(β) C-atoms have diameters of 4.0 and 5.4 Å, respectively. The corresponding values (from an X-ray structure) of an α-peptidic 3.6_{13}-helix are 3.6 and 4.7 Å (*cf. Fig. 1*).

helix than comparable β-peptides [21]. The intrinsic folding tendency of β-peptides is due to the fact that their backbone contains ethane moieties (*cf.* $NCH(R)-CH_2CO$ in a β^3-amino-acid residue), providing conformational stability through their preference for a staggered (*synclinal* or *antiperiplanar*) disposition of the substituents. In the extreme case, the *synclinal* or *gauche* dihedral angle around this $N-CHR-CHR-CO$ bond can be fixed – and the β-peptide 3_{14}-helix enforced – by incorporation into the cyclohexane ring of *trans*-2-aminocyclohexanecarboxylic acid [22].

The NMR analysis of the β^2/β^3-peptide **2** shows that equally charged side chains, *i.e.*, the $(CH_2)_4-NH_3^{\oplus}$ groups of the β^3hLys residues, can be placed in relative proximity without destroying the *10/12*-helical structure in MeOH. The charged Lys side chains also convey water solubility to compound **2**, so that we were able to measure the NMR spectra in H_2O. In this solvent, there was no single predominant conformation detected, confirming that the *10/12*-helix, which has no macrodipole [6–8], requires the helix-stabilizing solvent in the absence of conformational fixation, like the 3_{14}-helix.

In view of what was stated in the *Introduction*, it may be considered striking to see the full-length 3_{14}-helix of the icosapeptide **3** in MeOH solution, just like it was ten years ago when we saw a helix of a β-peptide consisting of as few as six residues [21] under the same conditions. The fact that the 20-mer helix does not appear to suffer from macrodipole destabilization may be taken as yet another piece of evidence for the importance of the staggered ethane bond in the backbone of β-peptides. The conformation-stabilizing effect of this element, which is present in each one of the 20 residues, seems to outweigh the destabilization by the macrodipole. Thus, we can conclude that both very short and very long β^3-peptidic 3_{14}-helices are much more stable than their natural counterparts under the same conditions (solvent, temperature). The present helix has a length of *ca.* 30 Å; we are now in the process of preparing somewhat longer β^3-peptides with aliphatic side chains along the major chain, and polar, cationic side chains near the termini, typical features of membrane-spanning peptides and protein sections. The aliphatic part of a phospholipid bilayer is *ca*. 40-Å thick, which will be spanned by eight 3_{14}-helical pitches of 5 Å each, corresponding to a 24-mer.

We thank Professor *Kurt Wüthrich*, Institute for Molecular Biology and Biophysics, ETH-Zürich, for providing high-field NMR-measuring time to acquire the data of the icosapeptide **3**. Financial support by *Novartis Pharma AG*, Basel, is gratefully acknowledged. Part of the results described herein was obtained in the course of the *Swiss Science Foundation* project SNF No. 200020-100182.

Experimental Part

Preparation of the α-Heptapeptide **1**. – Fmoc-Phe-Loaded *Wang* resin (0.1 g, 0.1 mmol) was used for coupling with the other six amino acids under standard conditions (see *Sect. 2* above). Removal from the resin ($CF_3COOH/(i\text{-}Pr)_3SiH/H_2O$ 95 : 2.5 : 2.5) gave the crude product **1**, which was purified by prep. reverse-phase HPLC: *Macherey-Nagel C8* column, UV detection. Yield of **1**: 55 mg (62%) as TFA salt. Colorless fluffy material, purity >98% (by anal. HPLC). CD (0.2 mM in MeOH): $-1.0\cdot10^4$ (232 nM); CD (0.2 mM in TFE): $-2.5\cdot10^4$ (226 nM), $-1.7\cdot10^4$ (205 nM); CD (0.2 mM in HFIP): $-9.6\cdot10^4$ (232.4 nM). IR (KBr): 3292*s*, 3067*s*, 2967*s*, 2622*w*, 2300*w*, 1661*s*, 1541*s*, 1457*m*, 1387*m*, 1366*m*, 1203*s*, 1138*s*, 1028*w*, 967*w*, 911*w*, 838*w*, 800*m*, 722*m*, 700*m*, 669*m*, 598*w*. NMR: see *Table 1*. MALDI-MS (2,5-dihydroxybenzoic acid) 822.4 (17, $[M+2\,Na-H]^+$), 802.4 (14), 801.4 (44), 800.4 (100, $[M+Na]^+$), 653.4 (12). HR-MS: 800.4361 ($C_{38}H_{63}N_7NaO_8S^+$; calc. 800.4351).

NMR Measurements. The trifluoroacetate salts (H_3N^+/COOH form) of β-peptides **1**–**3** were dissolved in CD_3OH (0.7 ml) and, for peptide **2**, H_2O/D_2O 9 : 1. The NMR spectra of **2** and **3** were acquired at 750 MHz (^1H)

Table 6. *NOE Distance Restraints for β-Icosapeptide* **3**

Residue	H-Atom[a])	Residue	H-Atom	Distance [Å]	Residue	H-Atom[a])	Residue	H-Atom	Distance [Å]
1	α_{Re}	1	β	2.9	2	HN	3	HN	3.4
2	β	2	γ	2.6	3	α_{Si}	4	HN	2.6
2	β	2	HN	2.9	4	α_{Re}	5	HN	2.5
2	γ	2	HN	3.0	4	HN	5	HN	3.3
3	β	3	α_{Re}	2.6	5	α_{Si}	6	HN	2.6
3	β	3	γ	2.5	6	α_{Si}	7	HN	2.7
3	β	3	HN	3.0	6	HN	5	HN	3.2
3	γ	3	HN	3.1	6	HN	7	HN	3.4
3	α_{Re}	3	HN	2.8	7	α_{Si}	8	HN	2.7
4	α_{Re}	4	β	2.7	7	HN	8	HN	3.2
4	α_{Re}	4	HN	2.9	8	α_{Si}	9	HN	2.6
4	β	4	HN	3.0	8	HN	9	HN	3.3
5	α_{Re}	5	HN	2.8	9	α_{Re}	10	HN	2.5
5	α_{Si}	5	β	2.6	9	HN	10	HN	3.3
5	β	5	γ	2.9	10	α_{Re}	11	HN	2.4
5	β	5	HN	2.9	10	α_{Si}	11	HN	2.6
5	γ	5	HN	3.0	10	HN	11	HN	3.2
6	γ	6	α_{Si}	2.7	11	HN	12	HN	3.2
6	γ	6	HN	3.4	12	α*	13	HN	2.5
6	α_{Si}	6	HN	3.0	12	HN	13	HN	3.4
7	α*	7	HN	2.9	13	α	14	HN	2.6
7	β*	7	HN	2.8	13	β	14	δ*	2.9
8	α_{Si}	8	HN	2.8	13	HN	14	HN	3.3
8	γ	8	β	2.7	14	α*	15	HN	2.6
8	HN	8	β	3.0	14	HN	15	HN	3.3
9	δ*	9	β	2.5	15	α	16	HN	2.5
9	HN	9	β	3.0	16	δ	15	α_{Re}	2.7
10	HN	10	α_{Si}	2.8	17	α_{Re}	18	HN	2.5
10	HN	10	γ	3.3	17	HN	16	α_{Si}	2.7
10	HN	10	β	2.9	17	γ	18	HN	3.7
11	α	11	β	2.8	17	HN	16	HN	3.3
11	γ	11	β	2.6	17	HN	18	HN	3.4
11	HN	11	β	2.9	18	α_{Re}	19	HN	2.6
11	HN	11	γ	2.8	19	HN	18	HN	3.4
12	HN	12	α*	2.6	2	γ	5	β	3.3
12	β	12	γ	2.7	2	HN	5	β	3.3
12	HN	12	γ	3.4	3	HN	1	α_{Si}	2.3
12	HN	12	α*	2.9	3	HN	5	β	3.1
13	β	13	α_{Si}	2.8	4	α_{Re}	7	β*	2.7
13	HN	13	α_{Si}	3.0	5	HN	7	β	3.1
13	β	13	γ	2.7	5	HN	8	β	3.2
13	β	13	HN	3.0	6	γ	9	δ*	4.6
13	γ	13	HN	2.8	7	β	4	HN	3.2
13	δ	13	HN	3.0	7	HN	10	δ	4.0
14	γ	14	α*	2.6	8	α_{Re}	11	β	2.6
14	β	14	α*	2.5	8	β	6	HN	3.2
14	HN	14	γ	3.1	8	HN	11	β	3.1
15	α_{Si}	15	δ	2.8	9	β	6	α_{Si}	2.8
15	β	15	γ	2.6	9	β	6	HN	3.1
15	β	15	HN	3.0	9	β	7	HN	3.3
15	α_{Si}	15	γ	2.8	9	HN	11	β	3.2
15	δ	15	HN	3.0	9	δ*	12	δ*	4.5

Table 6 (cont.)

Residue	H-Atom[a])	Residue	H-Atom	Distance [Å]	Residue	H-Atom[a])	Residue	H-Atom	Distance [Å]
15	γ	15	HN	3.1	10	β	7	α_{Re}	2.5
16	α_{Re}	16	HN	2.8	10	β	7	HN	2.9
16	α_{Si}	16	β	2.6	10	β	8	HN	3.0
16	HN	16	γ	3.0	10	HN	12	β	3.0
16	β	16	γ	2.7	11	β	8	γ	3.4
17	HN	17	α_{Si}	3.0	11	HN	13	β	3.1
17	α_{Re}	17	γ	2.7	11	HN	14	β	2.8
17	β	17	γ	2.5	11	γ	14	γ	5.0
17	β	17	HN	3.0	12	α*	15	β	2.5
17	γ	17	HN	2.9	12	β	9	α_{Re}	2.3
18	α_{Re}	18	β	2.6	12	HN	15	β	2.7
18	α_{Re}	18	HN	2.8	12	δ*	15	δ	4.5
18	β	18	HN	3.0	14	β	11	α*	2.5
19	α_{Re}	19	HN	2.8	14	γ	17	γ	3.5
19	α_{Re}	19	β	2.6	15	β	13	HN	3.3
19	HN	19	β	3.0	16	β	13	HN	3.0
19	HN	19	γ	3.3	16	γ	19	β	3.4
20	α_{Si}	20	β	2.9	16	HN	19	β	3.2
20	β	20	δ	2.9	17	HN	15	HN	3.5
20	β	20	γ	2.6	17	HN	19	β	3.3
2	α_{Si}	3	HN	2.7	18	β	15	δ	3.0
2	HN	1	α_{Re}	2.5	19	β	16	α_{Re}	2.6

[a]) α*, β* = pseudo-atom used for backbone CH_2; γ = pseudo-atom used for side chain CH_2 except for residues 10,13 and 15; δ* = pseudo-atom used for side chain CH_2 except for residue 16.

with presaturation of the solvent OH signal. DQF-COSY with coherence transfer selection by *z*-gradients. TOCSY with 100-ms mixing time. NOESY Spectra with mixing times of 150 and, for **3**, 400 ms. For β-icosapeptide **3**, HMBC and HSQC spectra with gradient coherence pathway selection were acquired with the spectral width in the ^{13}C-dimension reduced to include the aliphatic region only.

Spectra of α-heptapeptide **1** were acquired at 500 (^{1}H) and 125 MHz (^{13}C) with presaturation of the solvent OH signal. DQF-COSY with coherence pathway selection by *z*-gradients. TOCSY with 100-ms DIPSI-2 spin lock (8.9 kHz). HSQC and HMBC with coherence transfer selection by *z*-gradients. ROESY: clean ROESY [23] with 300- and 150-ms CW-spin lock (2.8 kHz). Spectral width 6000 Hz, $2k \times 512$ data points acquired (64 scans/FID) with TPPI. Processed with $\cos^2$ window function to give $1k \times 1k$ real data points. Polynomial baseline correction applied in both dimensions.

Assignments and volume integration of ROESY cross-peaks were performed with the aid of SPARKY [24]. Distance constraints and error limits were generated from cross-peak volumes by calibration with known distances (two-spin approximation, $\pm$20% error limits) through a python extension within SPARKY. The volumes of cross-peaks involving Me groups or other groups of isochronous H-atoms were corrected by division through the number of H-atoms.

Simulated-Annealing (SA) Structure Calculations. Program XPLOR-NIH v2.9.7 [25]. The standard parameter and topology files of XPLOR-NIH (parallhdg.pro; topallhdg.pro) were modified to accommodate β^3-amino acid residues. Minimized extended zigzag conformations were used as the starting structures. The SA calculation protocol (adopted from the torsional angle dynamics protocol of *Stein et al.* [26]) included 4000 steps (0.015 ps each) of high-temp. torsional angle dynamics at 20000 K, followed 4000 (0.015 ps) steps of slow cooling to 1000 K with torsion angle dynamics, 4000 steps (0.003 ps) of slow cooling to 300 K with Cartesian dynamics and a final conjugate gradient minimization. The only nonbonded interactions used were *Van der Waals* repel functions.

All *Figs.* representing calculated structures were generated with MOLOMOL v. 2K2 [27] and PovRay 3.6 (www.povray.org).

REFERENCES

[1] D. Seebach, A. K. Beck, D. Bierbaum, *Chem. Biodiv.* **2004**, *1*, 1111.
[2] R. L. Baldwin, G. D. Rose, *TIBS* **1999**, *24*, 26.
[3] R. L. Baldwin, G. D. Rose, *TIBS* **1999**, *24*, 77.
[4] R. L. Baldwin, *Biophys. Chem.* **1995**, *55*, 127.
[5] T. Soares, M. Christen, K. Hu, W. F. van Gunsteren, *Tetrahedron* **2004**, *60*, 7775.
[6] D. Seebach, K. Gademann, J. V. Schreiber, J. L. Matthews, T. Hintermann, B. Jaun, *Helv. Chim. Acta* **1997**, *80*, 2033.
[7] D. Seebach, S. Abele, K. Gademann, G. Guichard, T. Hintermann, B. Jaun, J. L. Matthews, J. V. Schreiber, *Helv. Chim. Acta* **1998**, *81*, 932.
[8] M. Rueping, J. V. Schreiber, G. Lelais, B. Jaun, D. Seebach, *Helv. Chim. Acta* **2002**, *85*, 2577.
[9] P. I. Arvidsson, J. Frackenpohl, D. Seebach, *Helv. Chim. Acta* **2003**, *86*, 1522.
[10] P. I. Arvidsson, N. S. Ryder, H. M. Weiss, G. Gross, O. Kretz, R. Woessner, D. Seebach, *ChemBioChem* **2003**, *4*, 1345.
[11] T. Kimmerlin, D. Seebach, *Helv. Chim. Acta* **2003**, *86*, 2098.
[12] A. De Capua, A. Del Gatto, L. Zaccaro, G. Saviano, A. Livigni, C. Gedressi, T. Tancredi, C. Pedone, M. Saviano, *Biopolymers (Peptide Science)* **2004**, *76*, 459.
[13] R. Aurora, G. D. Rose, *Protein Sci.* **1998**, *7*, 21.
[14] D. Seebach, P. E. Ciceri, M. Overhand, B. Jaun, D. Rigo, L. Oberer, U. Hommel, R. Amstutz, H. Widmer, *Helv. Chim. Acta* **1996**, *79*, 2043.
[15] T. E. Esfarjani, C. Hilty, K. Wüthrich, M. Rueping, J. V. Schreiber, D. Seebach, *Helv. Chim. Acta* **2002**, *85*, 1197.
[16] J. A. Kritzer, M. E. Hodsdon, A. Schepartz, *J. Am. Chem. Soc.* **2005**, *127*, 4118.
[17] A. Glättli, X. Daura, D. Seebach, W. F. van Gunsteren, *J. Am. Chem. Soc.* **2002**, *124*, 12972.
[18] T. Kimmerlin, D. Seebach, D. Hilvert, *Helv. Chim. Acta* **2002**, *85*, 1812.
[19] D. Seebach, J. V. Schreiber, P. I. Arvidsson, J. Frackenpohl, *Helv. Chim. Acta* **2001**, *84*, 271.
[20] D. F. Hook, P. Bindschädler, Y. R. Mahajan, R. Šebesta, P. Kast, D. Seebach, *Chem. Biodiv.* **2005**, *2*, 591.
[21] D. Seebach, M. Overhand, F. N. M. Kühnle, B. Martinoni, L. Oberer, U. Hommel, H. Widmer, *Helv. Chim. Acta* **1996**, *79*, 913.
[22] D. H. Appella, L. A. Christianson, I. L. Karle, D. R. Powell, S. H. Gellman, *J. Am. Chem. Soc.* **1996**, *118*, 13071.
[23] C. Griesinger, R. R. Ernst, *J. Magn. Reson.* **1987**, *75*, 261.
[24] T. D. Goddard, D. G. Kneller, Program SPARKY v3.110, University of California, San Francisco, 2004.
[25] C. D. Schwieters, J. J. Kuszewski, N. Tjandra, G. M. Clore, *J. Magn. Reson.* **2003**, *160*, 66.
[26] E. G. Stein, L. M. Rice, A. T. Brünger, *J. Magn. Reson.* **1997**, *124*, 154.
[27] R. Koradi, M. Billeter, K. Wüthrich, *J. Mol. Graphics* **1996**, *14*, 51.

Received April 27, 2005